The MOBY Cetacean Data Tag

Kristine Do, Ben Felson, Tiffany Qian, Sanjana Subramanian, Jakeb Tivey

The authors are with the Department of Mechanical Engineering, Columbia University, New York, NY (ktd2128@columbia.edu, baf2143@columbia.edu, tq2147@columbia.edu, ss6169@columbia.edu, jdt2176@columbia.edu). This material is based upon work developed in the MECE E3420 / E3430 Engineering Design Courses

***Abstract*— MOBY is a novel marine data tag that tracks the migration and behavioral patterns of whales. It is a minimally invasive, medium-term solution for marine research equipped with biomimetic suction cups, a self-aligning underwater camera, and a turbine-based regeneration system and speed sensor, which collectively work to enhance data collection and support extended research expeditions. The designed remora inspired suction cup removal force, molded from Vytaflex 40A, was greater than similar sized regular suction cups in dry, wet, and underwater environments with 95% confidence. For housing geometries, it was determined with 95% confidence that a wide body and tall fin resulted in the fastest pivot time to align to the current. A turbine design with 12 blades showed consistent angular velocity down to speeds of a coasting whale, generating 150 mA to support all onboard electronics and camera.**

I. Introduction

We aim to alleviate climate change by asking: how does nature already do it? One answer is whales. Whales sequester 33 tons of carbon in their lifetime, so protecting them could prove crucial for fighting climate change [1].

Current research employs invasive and noninvasive tagging methods, where a data collection device is attached to the whale via barbs or suction cups, respectively [2]. Challenges highlighted by leading marine researchers include deployment, orientation, and longevity [3]. Deployment involves using cumbersome boom arms or drones, which both suffer from imprecise placement due to maneuverability, timing, and turbulence. Tag orientation is difficult to control, impacting data usability, rendering video feeds useless, and adding time to data analysis. Existing tags lack longevity, lasting only 6 to 24 hours and requiring retrieval for data extraction, and invasive options sacrifice the comfort and health of the whale in order to stay on longer.

To address these issues, we created MOBY, a minimally invasive whale data tag to track migration paths, physiological data, and behavioral patterns. Its biomimetic remora suction array, inspired by remora fish, allows it to stay on a whale for a projected duration of up to 3 months. MOBY's onboard turbine uses the whale's motion to regenerate battery power, allowing the tag to stay perpetually charged. Its electronics system allows real-time, 5K video streaming and storage as well as providing temperature, humidity, pressure, GPS, and speed tracking data. Our user interface allows researchers to easily view live sensor and video data in the interim. Finally, its self-aligning housing uses the whale-induced current to align the housing and camera in the forward direction, providing the desired point-of-view video feed.

MOBY was designed with careful consideration of National Oceanic and Atmospheric Administration (NOAA) and Marine Mammal Science (MMS) guidelines for cetacean tags. For the remora inspired suction cups, various guidelines were considered during the design and prototyping process. According to the MMS, the suction must be as non-invasive as possible [4], and according to NOAA, the vacuum pressure of the suction can't be too strong or it may cause blistering [5]. For our self-aligning housing, a major design constraint was ensuring the tag's geometry and coating was smooth. According to NOAA, this reduces the drag felt by the whale and discourages unwanted attachment of other marine organisms. [5]. Finally, for the data collection of the sensors and cameras, we also folowed NOAA guidelines of how to best store and display data. This involved adopting specific naming conventions and UTC time-stamping to follow NOAA's underwater video protocols [6].

II. Methods

A. Remora Suction

All suction cups were initially modeled in SOLIDWORKS, turned into molds that were then 3D printed, and finally cast with silicone or rubber.

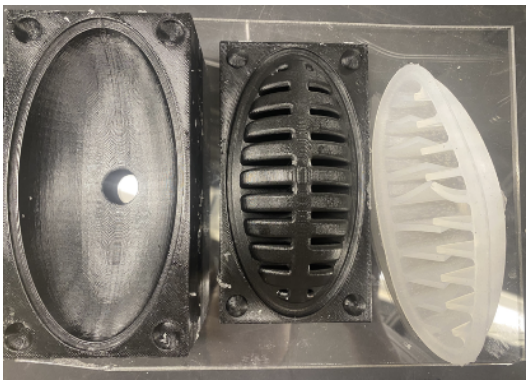

Fig. 1. 3D-Printed Mold and Remora Suction Molded with Ecoflex 00-31

There were three major materials that were tested in the iteration process. From softest to hardest on the Shore Hardness Scale, this included Ecoflex 00-31, a clear soft silicone, Vytaflex 40A, a beige rubber urethane, and Vytaflex 60A, a yellow rubber urethane [7].

Fig. 2. Top: Ecoflex 00-31 Remora, Bottom Left: Vytaflex 60A Regular, Bottom Right: Vytaflex 40A Remora

When molding the same remora suction out of the three materials, the clear Ecoflex 00-31 was too soft and unreliable in its suction, while the yellow rubber Vytaflex 60A was too rigid and not in line with NOAA practices, since its vacuum seal was strong enough that it pinched and required excessive force to compress. Thus, we picked Vytaflex 40A as an in between these two materials. Some preliminary pull tests between these prototypes showed that Vytaflex 40A better balanced the comfort of the suction cup to its strength. All final suction cups and testing were using Vytaflex 40A.

The major governing equation for suction cup vacuum forces is defined by equation 1,

$$F = P \times A \tag{1}$$

where F is the force of removal, and P and A are the pressure and area inside suction cup, respectively [8].

Iteration on the remora suction cup dimensions such as the width, length, and height, was done through trial and error and driven by housing geometry. Height was roughly always kept around two inches in order to ensure the suction cups would not experience higher drag forces. For the final analytical comparision, a regular suction cup of the same contact area of the final remora suction cup was molded using Vytaflex 40A. The suction pressures were all calculated using equation 1, left on the ballistic gel for extended period of time, and deemed to be safe for use.

Fig. 3. Regular Suction Cup Apparatus on Dry land

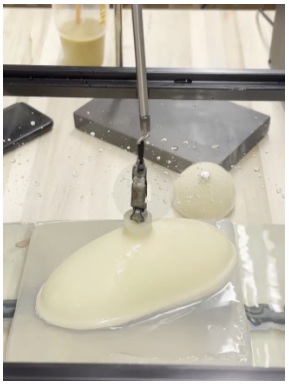

Fig. 4. Remora Suction Cup Apparatus in Wave Tank

To analyze the viability of the remora suction design, we performed a single-tailed t-test to see if the force to remove the remora suction cup was statistically greater than the force to remove the regular suction cup. Our null hypothesis, then, was that the force to remove the remora suction cup is not bigger than the force to remove the regular suction cup. We applied this null hypothesis to three different environments: (1) a dry surface, (2) a wet surface, and (3) underwater, the closest to a real world scenario where attachment happens on a wet surface but detachment happens underwater. We performed rigorous testing between the two in set-ups seen in Figures 3 and 4, and their removal forces were measured using a strain gauge on ballistic gel, the most commonly used whale skin analog [9].

B. Self-Aligning Housing

To address the design constraint of camera alignment, various housing geometries were tested in the wind tunnel [10]. Two features were varied to test for optimal tag alignment: tag width and fin height. This resulted in four 7-inch scaled down models, whose features are described in Table I. The 3D prints of said models are seen in Figure 5.

The first thing tested in the wind tunnel was pivot location. Five holes were drilled along the base of each 3D print and initial tests were performed in which the wind tunnel speed was increased incrementally until the tag aligned. It was decided that the second forward-most pivot location was optimal and all subsequent testing would be performed on that pivot location.

TABLE I
HOUSING GEOMETRY VARIATIONS

	Skinny Body	**Wide Body**
Short Fin	1	3
Tall Fin	2	4

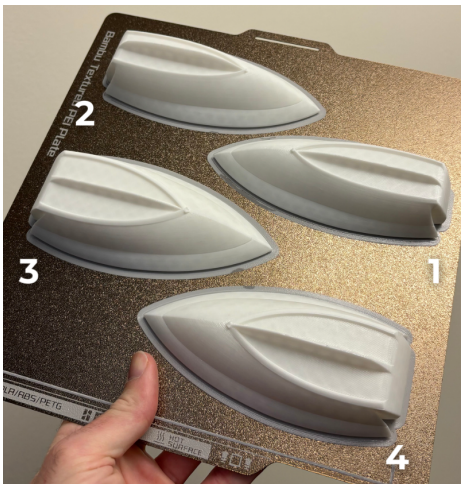

Fig. 5. 3D-Printed Housing Geometries

The testing apparatus comprised of a stand with a clamp attachment, as seen in Figure 6. The clamp held a collar by which a shoulder bolt could rotate freely about; said shoulder bolt was screwed into each tag geometry at pivot location two before each trial began.

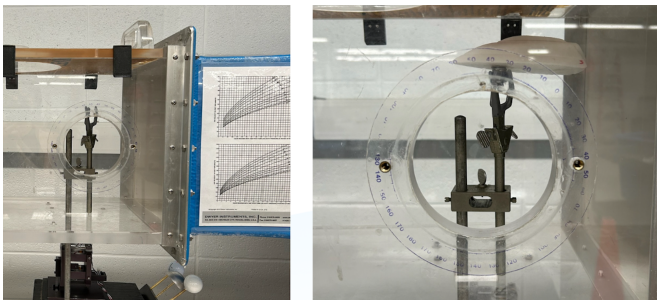

Fig. 6. Wind Tunnel Experimental Apparatus

Ten trials were conducted for each housing geometry variation, resulting in a total of 40 trials. To test the worst case scenario and thus the maximum alignment ability of each tag, each trial began with the tag rotated 180 degrees from the desired forward position. We then gradually increased the wind speed and recorded the minimum speed required to align the tag.

Histograms for the raw data of each subset were plotted to verify that all four sets followed a roughly normal distribution in order to ensure that an ANOVA test could be performed. To identify and exclude outliers for each 10 trial data set, we then performed Thompson Tau tests until outliers no longer remained. An ANOVA test was then performed on the cleaned datasets at a 95% confidence interval with a null hypothesis stating that the average minimum wind

speed for all geometries is statistically the same. To further compare the geometries, two-tailed t-tests were performed on all 6 subset pairs at the same confidence interval of 95%. The null hypothesis for the t-tests was that the average wind speed for Geometry A is statistically the same as the average wind speed for Geometry B.

C. Energy Regeneration

To allow MOBY to stay underwater for longer, an energy regeneration system was created. MOBY's dynamically orienting housing allows for water flow to optimally enter the turbine inlet.

A crossflow turbine apparatus was created consisting of a runner, nozzle, and draft opening. The runner was a cylinder with blades along its circumference. These blades could be horizontal, curved, or concave in shape to optimize different aspects of the flow. The nozzle directs water flow toward the runner at optimized angles. As the water flows onto the blades, its kinetic energy turns the runner, whose kinetic energy is converted into electrical current by a generator. Once water has flowed through the entire runner, it exits the turbine housing through the a draft opening in the turbine housing.

To successfully regenerate electricity, the turbine needed to steadily generate 150 mA—the maximum output of our generator when the whale is traveling 5 mph, an estimate of a whale's lowest travel speed [11]. A preliminary analysis was done using equation 2 to estimate power P produced by a turbine based on its geometrical parameters [12].

$$P = Q \cdot g \cdot \rho \cdot (H_g - H_l) \cdot \eta \tag{2}$$

where Q is the mass flow rate, g is the gravitational constant, ρ is the density of water, H_g is the distance the levels of water and turbine inlet, H_l is the loss of flow of water through joints or valves, and η is the efficiency of the turbine. The efficiency η was calculated with equation 3,

$$\eta = 0.5 \cdot C^2 \cdot (1 + \psi) \cdot \cos \alpha^2 \tag{3}$$

where C is a roughness parameter of the nozzle, which varies from 0.95 to 0.99, ψ is a coefficient representing the roughness of the blade, and α is the angle of attack.

In order to generate the best possible turbine design, several designs were simulated using SOLIDWORKS Flow Simulation. Each study was performed with the same parameters, varying only the design of the turbine and turbine housing, each one at a time, from study to study. The computational fluid dynamics (CFD) model requires a user to specify governing equations and parameters. In this study, the governing equations include the Navier-Stokes equations and a modified $k - \epsilon$ turbulence model with damping functions [13]. These sets of equations are discussed in further detail in V. Appendix.

The computational domain for these studies had the shape of a rectangular with a side lengths of 2 ft and height in the z-direction of 4 ft. Because the turbine housing is a rectangular prism of approximately 3 in x 3 in x 9 in, this computational domain is at least 5 times its respective length on the turbine. The boundary planes were adjusted such that the z-direction coincides with the direction of incident flow from the water. Water is set to flow in perpendicular to the opening in the turbine housing along this z-direction. A boundary condition is set with 5mph as a fluid inlet velocity. Water is assumed to be incompressible.

The computational mesh was subject to advanced channel refinement, where the mesh is optimized by refining regions of high-gradient flow and merging together regions of low-gradient flow. The refinement levels were considered for each study: coarse, medium, and fine. For mesh sensitivity analysis, a criterion was used such that analysis stops once a refinement of 50% leads to a difference in pressure of 0.01% or less. In every case except one, this threshold was reached with the medium mesh. Regardless, the finest mesh was used for all results to maintain the highest rate of accuracy.

For each design, the pressure and velocity of the water was measured at the geometric midpoints of the nozzle and the blade most aligned with the negative y-direction–the same direction as gravity. If a particular design change–for example, making the shape of the blades concave–increased the pressure and velocity of water at the inlet, then more design changes were made in the same spirit of the aforementioned change to further increase pressure and velocity. Design iteration was stopped once the inlet pressure and velocity were at least twice of the estimated threshold to produce 150 mA. This threshold was gathered from experimental data on the generator.

III. Results

A. Remora Suction

The final remora design is 5 inches long, 2.5 inches wide, and 1.25 inches tall. The final configuration has four regular suction cups on the outside and one remora suction cup in the middle, all molded from Vytaflex 40A. This improves upon the existing adhesion system in whale tags, but ensures that the product is still familiar enough for researchers to use.

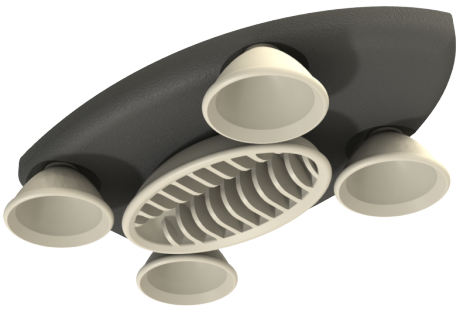

Fig. 7. Final Remora and Regular Suction Cup Layout on Tag Base

The forces to remove the remora suction cup and the regular suction cup in a dry surface, a wet surface, and underwater, as well as the respective experimental and alpha t-values are in Table II.

TABLE II

REMORA SUCTION VS. REGULAR SUCTION REMOVAL FORCES

	Remora Suction (N)	Regular Suction (N)	t_{exp}	t_{alpha}
Avg. Dry Removal Force (Normal)	86.81 ± 12.42	73.66 ± 6.30	4.2243	2.0478
Avg. Dry Removal Force (Tangential)	62.08 ± 13.21	43.20 ± 7.18	3.9700	2.1463
Avg. Wet Surface Removal Force (Normal)	69.97 ± 6.21	64.90 ± 8.26	2.1936	2.0295
Avg. Underwater Removal Force (Normal)	84.14 ± 16.14	63.66 ± 6.38	5.2778	2.0604

B. Self-Aligning Housing

The three fundamental requirements for an ANOVA test are normality, homogeneity of variance, and independence of observations. The latter two criteria were verified both in MATLAB and qualitatively, and the a roughly normal distribution was satisfied for all geometries, as shown in the histogram plots attained from plotting the raw wind tunnel data. These plots are displayed in Figures 11 through 14 in Appendix E.

After performing Thompson Tau tests to identify and exclude outliers, the mean minimum wind speeds required for alignment of the geometries defined in Table I were determined, as seen in Table III.

TABLE III

MEAN MINIMUM WIND SPEEDS

Geometry	Avg. Minumum Wind Speed (Hz)	Uncertainty (95%)
1	28.5 (23.9 m/s)	± 3.0
2	22.4 (18.5 m/s)	± 1.4
3	23.1 (19.2 m/s)	± 2.4
4	21.8 (18.0 m/s)	± 1.6

An ANOVA test was performed on the speeds for alignment for all housing geometries at 95% confidence, with the null hypothesis that all group means are statistically equal and a $F_{alpha} = 2.92$. The results can be seen in Table IV.

TABLE IV

ANOVA TEST COMPARING ALL HOUSING GEOMETRIES

DOF	Sum of Squares	Mean Sum of Squares	F_{exp}
3	258.73	86.243	10.598
32	260.41	8.1378	—
35	519.14	—	—

Individual two-tailed t-tests were done at 95% confidence, with a $t_{alpha} = 2.1199$ for all six combinations of housing geometries. The results can be seen in Table V.

TABLE V

T-TESTS FOR ALL HOUSING GEOMETRY COMBINATIONS

Geometry	2	3	4
1	t_{exp12} = 4.3164	t_{exp13} = 3.2949	t_{exp14} = 4.5786
2	—	t_{exp23} = -0.5868	t_{exp24} = 0.5901
3	—	—	t_{exp34} = 1.0067

Ultimately, from the results seen in Tables III through V, it was decided that a geometry like number 4, comprising a wide body and tall fin, would be most ideal for MOBY applications. The final housing was finalized to have a length of 10 in and a width of 7 in, with a fin height of 1.5 in and can be seen in Figure 8.

Fig. 8. Final Self-Aligning Housing Design

C. Energy Regeneration

The final design of the turbine blades is seen in Figure 9 and that of the turbine housing is seen in Figure 10. From the study created, aforementioned measured points had an average velocity of 254.25 $\frac{\text{in}}{\text{s}}$, or 14.44 mph, and an average pressure of 16.78 $\frac{\text{lb}}{\text{in}^2}$.

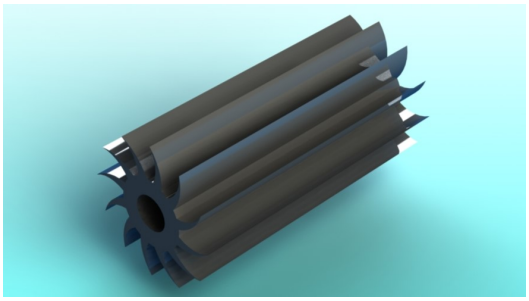

Fig. 9. Final Turbine Runner and Blade Design

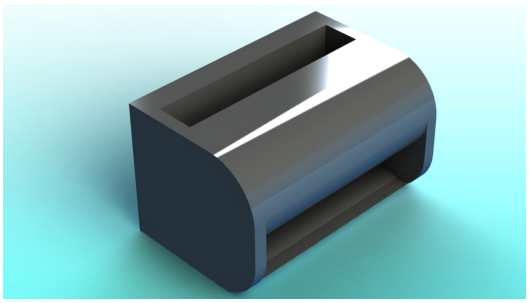

Fig. 10. Final Turbine Housing Design

IV. DISCUSSION & CONCLUSION

A. Remora Suction

For all three environments, dry, wet, and underwater, $t_{alpha} < t_{exp}$. Thus, at 95% confidence, we were able to reject the null hypothesis, showing the force to remove the remora suction cup is statistically greater than the regular suction cup. This means that the added remora suction cup does improve upon the existing suction cups, and having it on the tag will increase the longevity of the tag on the whale. Most importantly, from Table II, the difference between the t_{exp} and t_{alpha} value is the greatest in the last row, the average underwater removal force. This means that the

remora suction tag will outperform the regular suction cups the most in underwater conditions, which is the closest to real-life conditions in the field.

The strain-gauge and ballistic gel apparatus successfully tested the suction force, showing the design improves upon the current suction system, as well as having a safe vacuum pressure in line with NOAA and MMS standards [4] [5]. However, some possible errors in the results could have come from inconsistent temperature, humidity, or surface conditions, as well as human error when operating such as not pulling perfectly normal or tangential to the suction cup. These variation errors were accounted for by doing the pull tests in the same day by one person, deploying the suction cups the same way, and drying and cleaning the suction cups and ballistic gel when switching between environments to ensure a consistent baseline.

A major shortcoming of the testing method is the lack of long-term testing that we were able to do, both at the proper depths and varying flow speeds; this was due to lack of proper equipment and ability to simulate the ocean environment. Another area of future work for our remora-inspired suction is introducing a skin-safe barnacle bio-cement as a way to further improve the longevity of the tag. With more time and greater budget, we would test the suction at length and in the field, allowing us to be more confident in the success of this novel adhesion system.

B. Self-Aligning Housing

Results from the ANOVA test allowed us to conclude that at a 95% confidence, there is sufficient evidence to reject the null hypothesis since $F_{exp} > F_{alpha}$ and thus, we can conclude that varying the geometry of MOBY does indeed have an effect on its alignment ability.

Results from the two-tailed t-tests revealed that at 95% confidence, the mean minimum wind speed of alignment was statistically the same for all geometries, except Geometry 1. This is exemplified by the t-values in Table V, where $t_{exp12} > t_{alpha}$, $t_{exp13} > t_{alpha}$, and $t_{exp14} > t_{alpha}$, meaning there is sufficient evidence to reject the null hypothesis of mean equality. Meanwhile, all combinations comprising Geometries 2 through 4 resulted in $t_{exp} > -t_{alpha}$ and $t_{exp} < t_{alpha}$, meaning there is insufficient evidence to reject the null hypothesis and the mean wind speeds for Geometries 2 through 4 are statistically the same. Qualitatively, this means that a housing geometry with a skinny body and short fin is undesirable since, as seen in Table III, that combination of fin height and body width resulted in the highest mean wind speed required for alignment.

With this in mind, we then compared mean values for Geometries 2 through 4. The average wind speed for Geometry 4 was the lowest out of the three and empirically, it was observed during testing that a wide geometry offered more stable results; in general 3 and 4 out-performed their narrow counterparts. Furthermore, although only slightly lower, the mean wind speeds for 2 and 4, when compared to the short fin geometries, also indicate that a taller fin offers better alignment ability. Ultimately, we concluded that a housing with the features of Geometry 4 would best support modular electronics and optimized alignment.

Using the wind tunnel data sheet given by the Columbia University Mechanical Engineering Teaching Lab, we were able to extrapolate and convert the attained mean wind speeds from Hz to m/s. We then verified, via the dimensional analysis between water and air derived in Appendix D, that the wind speed required to align the tag was well below the current induced by the coasting speed of a whale. Thus, we are confident that the tag would be able to reorient itself in the forward direction using whale-induced current.

Some shortcomings the wind tunnel tests resulted from the experimental setup. It was difficult to accurately screw the shoulder bolt into each tag geometry exactly the same way for each of the 40 trials. Some error and inconsistencies in the data likely resulted from this. Moreover, if we were to repeat the testing, a more drastic difference in fin height and tag width would likely allow for more clear, definitive differences in performance between the four geometries. Time permitting, we could have tested our final large scale model seen in Figure 8 to ensure alignment ability.

Ultimately, the dream goal for our novel self-aligning housing would be to professionally manufacture it with pressure and depth graded materials, ensuring waterproofing ability and durability and finally, testing it in the field.

C. Energy Regeneration

After much iteration, the final design has 12 blades—enough where water keeps the turbine running at a consistent angular velocity without crowding the inlet so much that the effective surface area of the blade is reduced. Each blade has the same geometry, consisting of two arcs at different radii connected to the runner. The arcs connect together on the outside of the runner, creating a sharp blade shape.

Interestingly, changing the geometry of the turbine housing had a qualitatively larger effect on inlet pressure and velocity than the actual shape of the blades.

Internally, the chamber is very slightly larger than the runner and blades for tolerance purposes. The inlet of the turbine has a larger area than the nozzle feeding to the runner to increase velocity. Additionally, a small "lip" can be seen at the bottom of the inlet, serving the same purpose. Finally, the outlet area is smaller than the nozzle, causing fluid to flow more quickly through the runner. Externally, fillets were used to allow fluid that doesn't go through the runner to flow easily around the housing, reducing the shear force on the tag and therefore the likelihood of detachment from incident flow.

Several structural parts were later added to the turbine housing, but are located on the sides. While the design challenges for these parts were interesting, they did not warrant quantitative analyses, nor did they affect the flow profile, inlet pressure, and inlet velocity.

Several potential shortcomings exist within the analysis conducted to optimize turbine design. The assumption that water is an incompressible fluid in our CFD simulations is largely insignificant since including compressibility in our

analysis would likely not change the results much, and would introduce lots of complexity. One large discrepancy between analysis and reality is the fact that CFD simulations were done with a uniform flow as opposed to a turbulent flow, more closely resembling the real world. The idea behind choosing uniform flow was that turbulent flow would still align with incident flow, and would thus make the turbine turn more quickly, only making it more effective. By analyzing a uniform flow, we come up with a more conservative estimate for inlet pressure and velocity. Additionally, we assume water will not enter through the draft opening unless a significant event reverses the water flow direction.

CFD simulations—as all models—are inherently wrong. To address this fact, the CFD simulations were used as design inspiration, rather than as justifications for specific inlet pressures or velocities. While it can be helpful to produce a single number after an analysis, it was more helpful to use the simulations as a gauge on how well a design might perform compared to other designs.

To better test and quantify turbine designs, an experiment could have been set up in a wind tunnel or a flow tank, and the turbine angular velocity measured. Essentially, we could have done the experiment in person instead of on a computer. Because the turbine itself is quite small, and getting equipment to fit inside it and calibrating it accurately would cost lots of time and money, it was not included in the scope of this analysis. Additionally, although it would have been more accurate, testing turbine designs in person would not have allowed as rapid of iteration and comparison as CFD studies.

In a perfect world, a study where our electronics array tracked the current input while MOBY was atop a whale would have been a perfect test. Seeing how the turbine reacted in the real world would have likely led to problems to address, potentially including waterproofing of wires, the turbine rotating too quickly, or shear forces. While these factors were considered in this analysis, they could not have been accurately simulated with CFD.

D. Conclusion

MOBY represents a comprehensive and innovative approach to cetacean research, providing optimal tracking of whale migration and behavioral patterns through its state-of-the-art design and engineering solutions.

By equipping MOBY with an adhesion array with a novel Remora suction cup made from Vytaflex 40A, the tag can maintain a more secure attachment to whales for longer periods of time. This was demonstrated at 95% confidence using t-tests to require more force to remove than regular suction cups. Moreover, MOBY's self-aligning wide body and tall fin housing design was tested in a wind tunnel, and shown with 95% confidence in ANOVA tests to quickly realign to incident flow. This alignment design enhances the quality and orientation of video footage, providing much needed insight into whale behavior and migration patterns. Additionally, MOBY's onboard regenerative turbine enables efficient battery power regeneration from the whale's natural motion at coasting speeds, capable of consistently producing a 150 mA current. This ensures the sustainability and extended operation of MOBY's onboard electronics, supporting longer data collection periods and as it remains on the back of the whale.

We have implemented thoughtful and empathetic design decisions, and we are confident that MOBY is ready to advance the worlds of whale research and climate change. Through MOBY, researchers can gain deeper insights into whale behavior, migration, and conservation needs, ultimately contributing to the protection and understanding of these vital species.

V. Appendix

A. Modified $k-\epsilon$ Turbulence Model

The modified $k-\epsilon$ turbulence model with damping functions was proposed by Lam and Bremhorst [14] to describe flows of homogeneous fluids which abide by the following conservation laws:

$$\frac{\partial \rho k}{\partial t} + \frac{\partial \rho k u_i}{\partial x_i} = \frac{\partial}{\partial x_i}\left(\left(\mu + \frac{\mu_t}{\sigma_k}\right)\frac{\partial k}{\partial x_i}\right) + C_{\epsilon 1}\frac{\epsilon}{k}\left(f_i \tau_{ij}^R \frac{\partial u_i}{\partial x_j} + C_B \mu_t P_B\right) - f_2 C_{\epsilon 2}\frac{\rho \epsilon^2}{k} \quad (4)$$

$$\tau_{ij} = \mu s_{ij} \quad (5)$$

$$\tau_{ij}^R = \mu_t s_{ij} - \frac{2}{3}\rho k \delta_{ij} \quad (6)$$

$$s_{ij} = \frac{\partial u_i}{\partial x_j} + \frac{\partial u_j}{\partial x_i} - \frac{2}{3}\delta_{ij}\frac{\partial u_k}{\partial x_k} \quad (7)$$

$$P_B = -\frac{g_i}{\sigma_B}\frac{1}{\rho}\frac{\partial \rho}{\partial x_i} \quad (8)$$

where

- $C_\mu = 0.09$
- $C_{\epsilon 1} = 1.44$
- $C_{\epsilon 2} = 1.92$
- $\sigma_k = 1$
- $\sigma_\epsilon = 1.3$
- $\sigma_B = 0.9$
- $C_B = 1$ if $P_B > 0$, $C_B = 0$ if $P_B < 0$

Turbulent viscosity is found by

$$\mu_t = f_\mu \frac{C_\mu \rho k^2}{\epsilon} \quad (9)$$

where

$$f_\mu = \left(1 - e^{-0.025 R_Y}\right)^2 \left(1 + \frac{20.5}{R_t}\right) \quad (10)$$

where

$$R_Y = \frac{\rho \sqrt{k} y}{\mu} \quad (11)$$

$$R_t = \frac{\rho k^2}{\mu \epsilon} \quad (12)$$

B. Navier-Stokes Equations

The Navier-Stokes equations are laws describing mass, momentum, and energy conservation of fluids [13]. They are the governing equations for the CFD analyses performed on the regenerative turbine.

$$\frac{\partial \rho}{\partial t} + \frac{\partial (\rho u_i)}{\partial x_i} = 0 \tag{13}$$

$$\frac{\partial (\rho u_i)}{\partial t} + \frac{\partial}{\partial x_j}(\rho u_i u_j) + \frac{\partial P}{\partial x_i} = \frac{\partial}{\partial x_j}(\tau_{ij} + \tau_{ij}^R) + S_i \tag{14}$$

$$\frac{\partial \rho H}{\partial t} + \frac{\partial \rho u_i H}{\partial x_i} = \frac{\partial}{\partial x_i}(u_j(\tau_{ij} + \tau_{ij}^R) + q_i) + \frac{\partial p}{\partial t} - \tau_{ij}^R \frac{\partial u_i}{\partial x_j} + \rho\epsilon + S_i u_i + Q_H \tag{15}$$

$$H = h + \frac{u^2}{2} \tag{16}$$

C. Uncertainty Analysis

For all tests bias and precision uncertainties were considered for each measured value. The total uncertainty combines both bias and precision uncertainties and is defined by equation 17 and represented as U_{N_i} in equation 18.

$$U_N^2 = \sqrt{B^2 + P^2} \quad (15) \tag{17}$$

$$U_E^2 = U_{N_1}^2 \left(\frac{\partial E}{\partial N_1}\right)^2 + U_{N_2}^2 \left(\frac{\partial E}{\partial N_2}\right)^2 + \ldots + U_{N_i}^2 \left(\frac{\partial E}{\partial N_i}\right)^2 \tag{18}$$

D. Dimensional Analysis

To simulate the same Reynolds number (Re) for flows in different media, we use equation 19:

$$\mathrm{Re} = \frac{\rho V L}{\mu} \tag{19}$$

where

- ρ: fluid density (kg/m^3),
- V: flow velocity (m/s),
- L: characteristic length (m),
- μ: dynamic viscosity (Pa·s).

For equal Reynolds numbers in water and air, assuming equal L, the velocities relate as:

$$\frac{\rho_{water} \cdot V_{water}}{\mu_{water}} = \frac{\rho_{air} \cdot V_{air}}{\mu_{air}} \tag{20}$$

Given $\rho_{\text{water}} \approx 1000$ kg/m^3, $\rho_{\text{air}} \approx 1.225$ kg/m^3, $V_{\text{water}} = 4$ m/s, $\mu_{\text{water}} \approx 1 \times 10^{-3}$ Pa·s, $\mu_{\text{air}} \approx 1.8 \times 10^{-5}$ Pa·s, the air velocity V_{air} can be calculated by equation 21:

$$V_{\text{air}} = V_{\text{water}} \frac{\rho_{\text{water}} \cdot \mu_{\text{water}}}{\rho_{\text{air}} \cdot \mu_{\text{air}}} \tag{21}$$

E. Wind Tunnel Testing Data

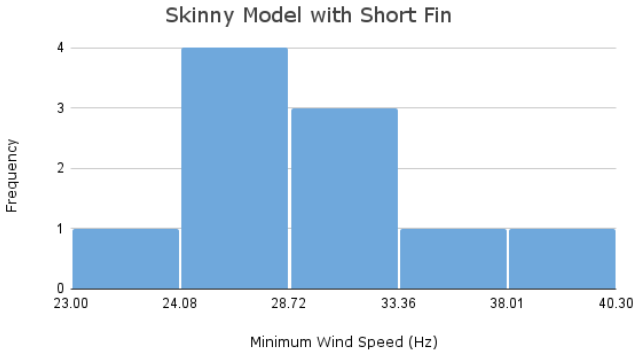

Fig. 11. Histogram for Housing Geometry 1

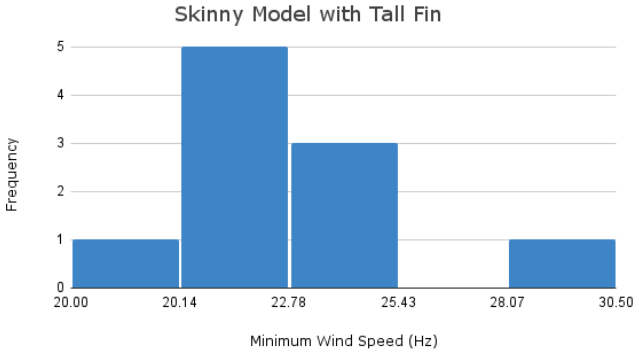

Fig. 12. Histogram for Housing Geometry 2

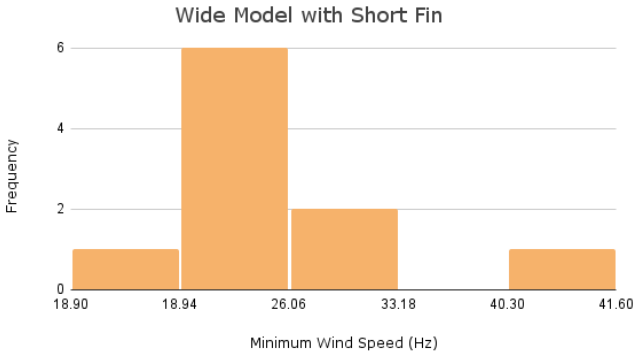

Fig. 13. Histogram for Housing Geometry 3

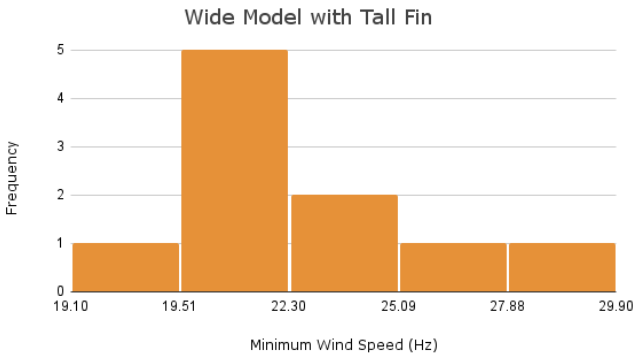

Fig. 14. Histogram for Housing Geometry 4

REFERENCES

[1] O. of Protected Resources, "Whales and carbon sequestration: Can whales store carbon?," 2024.

[2] K. McPherson, "Tagging right whales: Know your tag types," 2023.

[3] O. of Protected Resources, "A whale's perspective: Using tags to understand north atlantic right whales," 2023.

[4] N. J. Gales, W. D. Bowen, D. W. Johnston, and K. M. Kovacs, "Guidelines for the treatment of marine mammals in field research," *MARINE MAMMAL SCIENCE, VOL. 25, NO. 3*, 2009.

[5] R. D. Andrews, "Best practice guidelines for cetacean tagging," *J. CETACEAN RES. MANAGE 20: 27–66*, 2019.

[6] D. Coleman and S. A. Soule, "Establishing community standards for underwater video acquisition, tagging, archiving, and access," 2016.

[7] A. Products, "Durometer shore hardness scale explained," 2020.

[8] E. V. Technologies, "How to calculate vacuum suction force?," 2022.

[9] D. N. Wiley, C. J. Zadra, A. S. Friedlaender, S. E. Parks, A. Pensarosa, K. A. Shorter, J. Urbán, and I. Kerr, "Deployment of biologging tags on free swimming large whales using uncrewed aerial systems," *R Soc Open Sci.*, 2023.

[10] K. Hoffmann, J. T. Rasmussen, S. O. Hansen, M. Reiso, B. Isaksen, and T. E. Aasland, "The use of wind tunnel facilities to estimate hydrodynamicdata," *EPJ Web of Conferences 114, 02040*, 2016.

[11] R. Paros, "10 facts you didn't know about north atlantic right whales," 2018.

[12] B. A. Nasir, "Design considerations of micro-hydro-electric power plant," *Energy Procedia 50*, 2014.

[13] D. A. Sobachkin and D. G. Dumnov, "Numerical basis of cad-embedded cfd," 2014.

[14] C. Lam and K. Bremhorst, "A modified form of the k-e model for predicting wall turbulence," *Transactions of the ASME*, 1981.

ACKNOWLEDGEMENTS

The MOBY team would like to thank the following marine researchers and Columbia faculty and staff for their contributions and support throughout the duration of this project. The researchers we worked with have an immense passion for their work that inspired our own passion for cetacean research. They received our questions with an openness and enthusiasm that fostered a collaborative and interdisciplinary environment.

- **Charles "Stormy" Mayo**—Program Director, Center for Coastal Studies
- **Chris Zadra**—Drone Programs Manager, Ocean Alliance Inc.
- **Christy Hudak**—Research Associate, Center for Coastal Studies
- **Dave Cade**—Active Researcher, Stanford University & Oregon State University
- **Leigh Torres**—Marine Ecologist & Associate Professor, Oregon State University
- **Mauricio Cantor**—Behavioral Ecologist, Oregon State University
- **Monica Ross**—Senior Research Scientist, Clearwater Marine Aquarium
- **Kristin Myers**—Associate Professor of Mechanical Engineering, Columbia University
- **Yevgeniy Yesilevskiy**—Lecturer of Mechanical Engineering, Columbia University
- **Mechanical Engineering Teaching Lab Staff**
- **Barnard Design Center Staff**